RESEARCH ARTICLE OPEN ACCESS

Numerical Study of Star Anchor Plate Embedded in Cohesive Soil

R. Djamaluddin*, L. Samang*, A.M. Imran**, A.B. Muhiddin*
*Departement of Civil Engineering Hasanuddin University, Makassar 90245, Indonesia
**Departemant of Geological Engineering Hasanuddin University, Makassar, 90245, Indonesia

ABSTRACT: Indonesia as an archipelago country has a very long coastline about 90.000 kms. Specifically for shore and offshore, there are many buildings utilizing structures including floating deck, mooring dolphin, offshore platforms etc. Those requires a solution to maintain the stability of the structures due to the vertical movement of tides and horizontal movement of currents, wind and waves. To maintain the stability due to buoyant force, structure of anchors are needed. Various types of the anchor have been widely used such as drag, helical, anchor plate circular shape and square. This study aims to do the development of new modifications of a plate anchor type star with 4 leaves with an area of a fixed and diameter equivalent different on any variations. Ultimate pullout capacity was obtained by using numerical geomechanics analysis within finite difference method. A perfectly plastic soil model was used with a tresca yield criterion. Results are presented including break-out factors based on various anchor shapes and embedment depth. Our findings are also compared with previous numerical and empirical solutions.

Keywords: Pullout Capacity, Star Plate, Anchor, Clay Soil, Break-out Factors.

I. INTRODUCTION

Anchors have been developed for various purposes such as strengthening the slopes, retaining walls (plaster), the stability of the tunnel, the foundation for preventing transmission tower style pull, roll, etc. There are many types of anchors depending on the type of load and large, the type of structure and local subsoil conditions. The behavior of anchors in the field indicate that the collapse mechanism and bearing capacity of the anchor can be determined by many factors. Most studies focus on massive models shaped anchor plates with various shapes (circle, square) with a variation of the dimensions, depth, and type of load.

Some studies have been conducted on anchor plates. Merifield et. al (2003) examined numerically the anchor plate circle, square, and strip solutions with the lower bound method. The development forms an anchor element with easy installation and sufficient carrying capacity. A study conducted by Djamaluddin et al. (2013) introducing anchor element type star shape embedded on cohesive compacted soil through an experimental laboratory. They investigated a pull-out capacity, collapse models, and displacement due to the effect of: (1) the area of the anchor plate with a fixed diameter, (2) wide diameter anchor remains unchanged, and (3) variations in the depth of embedment. However, numerical studies for this type of anchor has not yet been done to validate the experimental model that have been carried out in the laboratory. This paper presents numerical analysis of star anchor embedded in clay soil by using finite difference.

II. NUMERICAL METHOD

Engineering problems in Geomechanics and Geotechnical fields are commonly treated through the infinite or semi-infinite media. The best approach to solve these problems numerically is by coupling a finite element or a finite difference with boundary element numerical methods. Coupling the bounded domain modelled by Flac3D (Itasca, 2005), a well-known program that implements an explicit finite difference method, with the boundary element method, which satisfies exactly the governing Partial Differential Equations (PDE) in the surrounding infinite or semi-infinite medium, combines the capabilities and the advantages of both methods.

Anchors are typically constructed from steel or concrete and may be circular (including helical), square, or rectangular in shape. This study aimed to do the development in the form of modifications plate anchor circular becoming a plate anchor type star with 4 leaves with an area of a fixed and diameter equivalent different on any variations shown in Figure 1.

A general layout of the problem to be analyzed is shown in fig. 2(a) and star anchor layout of the problem to analyzed is shown in fig. 2 (b). The analysis of anchor behavior may be divided into two distinct categories, namely those of “immediate breakaway.” And “no breakaway.” Rowe and Davis (1982). The analaysis in this paper are for the immediate breakaway case only.

Anchor can be classified as shallow or deep, depending on their mode of failure. This point is illustrated in Figure 3. An anchor is classified as

shallow if, at ultimate collapse, the observed failure mechanism reaches the surface. In contrast, a deep anchor is one whose failure mode is characterized by localized shear around the anchor and is not affected by the location of the soil surface.

For a given anchor size, B, and soil properties ɣ, cu their exist a critical embedment that Hcr at which the failure mechanism no longer extend to the soil surface. This type of failure mechanism is typically observed for deep anchor, and is localized around the anchor. The significance of such localized failure mechanism is that the ultimate capacity of the anchor will have reached a maximum limiting value. This arises because the undrained shear strength is assumed to be independent of the mean normal stress.

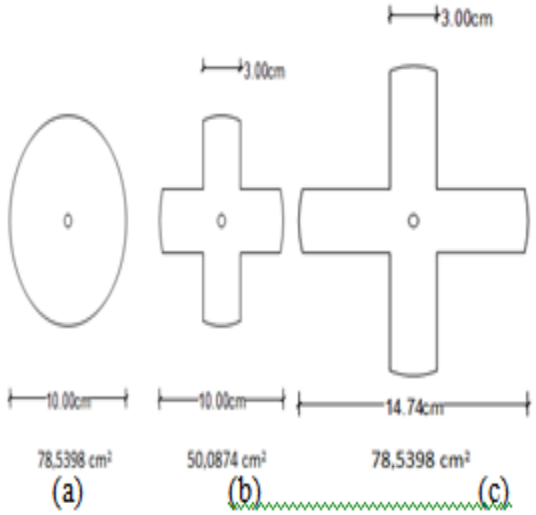

Figure 1. Type notation of star plate anchor (a) circular, (b) star A, and (c) star B

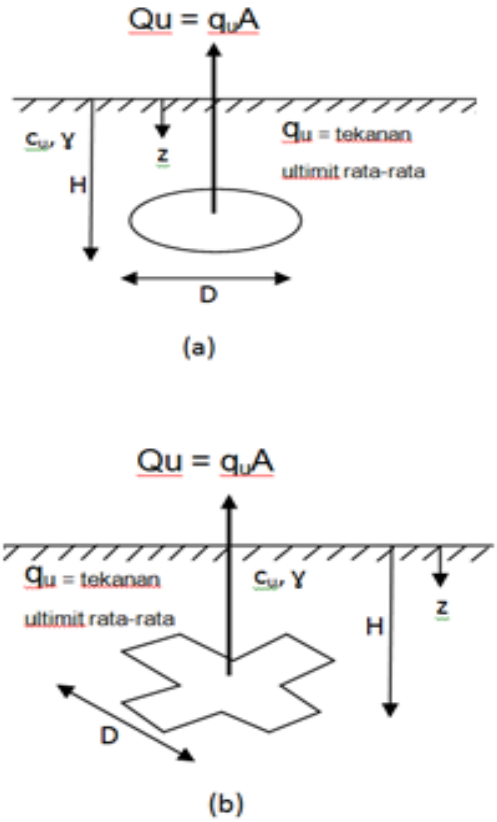

Figure 2. Problem notation of star plate anchor (a) circular, and (b) star A and star B

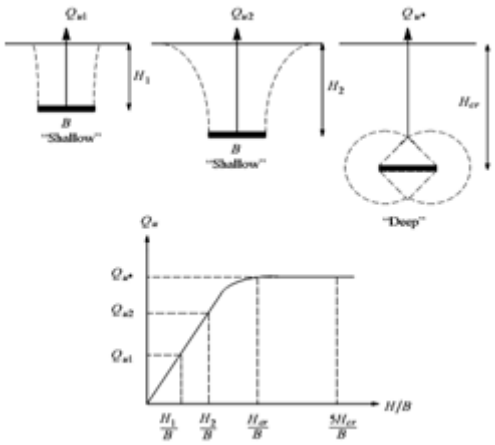

Fig. 3. Shallow and deep anchor behavior.

2.1 Pull-out capacity of anchors in undrained clay

Ultimate pull-out capacity of anchors in clay undrained conditions proposed by Merifield et al. (2003), are usually shown as a function of undrained shear strength in the following form.

$$q_u = \frac{Q_u}{A} = c_u N_c \qquad (1)$$

where A = the anchor area, c_u = the undrained soil strength at the ground surface, and N_c = anchor break-out factor.

For convenience, Merifield et. al (2003) has been defined the anchor break-out factor for the following two cases:

1. For a homogeneous soil profile with no unit weight ($\gamma = 0$)

$$N_c = N_{co}, \text{where } N_{co} = \left(\frac{q_u}{c_u}\right)_{\gamma=0} \quad (2)$$

2. For a homogeneous soil profile with unit weight ($\gamma \neq 0$)

$$N_c = N_{c\gamma}, \text{where } N_{c\gamma} = N_{co} + \frac{\gamma H}{c_u} \quad (3)$$

Eqs. (1)- (3) reflect the complex nature of the break-factor n_c observed by Rowe and Davis (1978). The break-out factor is a functional of embedment ratio (H/B) and overburden pressure, with the latter being expressed in term of dimensionless quantity $\gamma H/c_u$. this indicates that, separate from overall problem geometry, the soil property directly influence anchor behavior.

It should be noted that the break-out factor given in eqs. (1) –(3) does not continue to increase indefinitely, but reaches a limiting value which marks the transition between shallow and deep anchor behavior. The limiting value of the break-out factor is defined as Nc*.

Implicit in eqs. (3) is the assumption that the effect of soil unit weight and cohesion are independent of each other and may be superimposed. This assumption was investigated in the previous study of Merifield et. al. (2005), where it was found that the principle of superposition can be successfully applied to shallow strip anchors in clay.

2.2 Three dimensional modeling details

A simplified representation of the boundary grid arrangements used to analyzed circular, star A, and star B anchors illustrated in fig. 4 and 5. The soil mass is first discretized into a number of zone where the boundaries between adjacent zone may be specified as a stress discontinuity or rigid joint. Each zone is then subdivided in three-dimensional space to form a number of radial cylinder grid for circular anchor and brick grid for star anchor within each zone. To model a smooth anchor may be modeled by insisting the shear stress is zero at all element nodes along the anchor. To allow the under side of the anchor to separate from the soil (immediate breakaway), the stress discontinuity between the zone above the anchor segment is removed, and the shear stress and normal stress are force to be equal to zero.

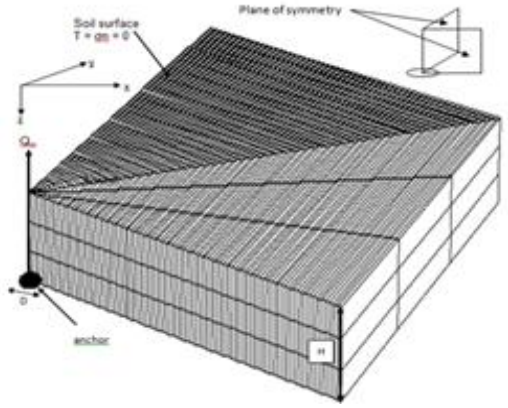

Figure 4. Typical grid used for analyzing of circular anchor

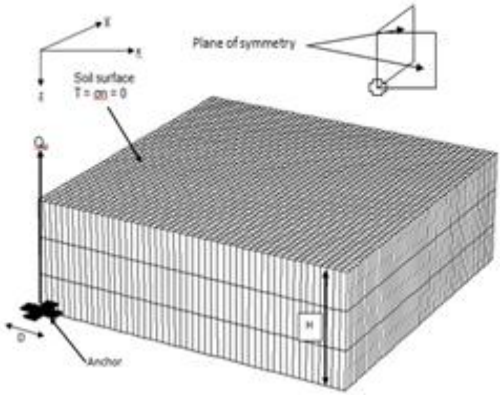

Figure 5. Typical grid used for analyzing of star anchor

III. DISCUSSION

3.3 Break-out factor

Numerical analysis of the anchor break-out factor N_{co} in clay are shown in Fig. 6. These break-out factors were compared with those obtained for circular, star A, and star B anchors by Djamaluddin et al. (2013). The break-out factor N_{co} was found to increase steeply before reaching a constant value at H/D ≈ 7, approximately 14.3 for circular anchor, 20.5 for star A anchor, and 15.6 for star B anchor. It is also shown in Fig. 6, Merifield et. al (2003) found that the break-out factor N_{co} was found to increase steeply before reaching a constant value at H/D ≈ 7, approximately 12.56 for circular anchor. However, the solution derived by Meyerhof et. al (1968), the break out factor increase linearly. The laboratory tests indicates that the break-out factor N_{co} was found to increase steeply before reaching a constant value at H/D ≈ 7, approximately 14.1 for circular anchor, 20.4 for star A anchor, and 15.8 for star B anchor.

3.2 Shape factor

These shape factors have been compared with those obtained for circular, star A, and star B anchors as shown in Fig. 7. The shape factor *S* was found to increase steeply before reaching a peak value at H/D ≈ 6.8, approximately 2.16 for circular anchor, 3.08 for star A anchor, and 2.36 for star B anchor. Merifield et. al (2003) suggested that the shape factor S value decreases steeply at H/D 3 to 9, approximately 1.95 to 1.7 for circular anchor. Yet, it was found that the shape factor S value increases almost linearly, at H/D 3 to 9, approximately from 0.8 to 1.22 for circular anchor. The laboratory tests by Djamaluddin et al. (2013), shown in Fig 7, shape factor S increases significantly at a peak at H/D ≈ 6.8, approximately 2.14 for circular anchor, 3.08 for star A anchor, and 2.32 for star B anchor.

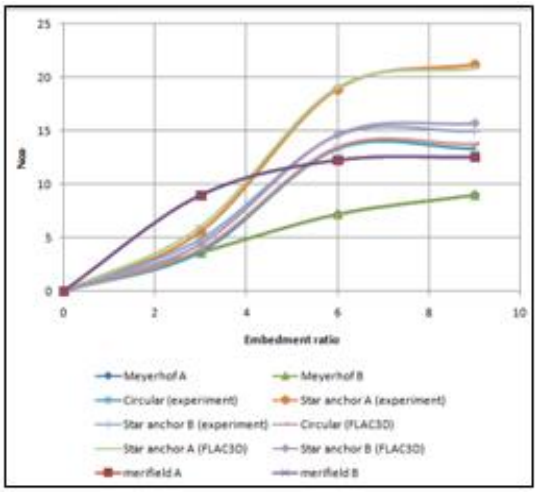

Figure 6. Comparison Break-out factors anchors in clay

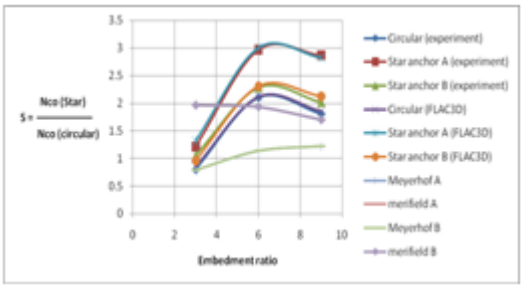

Figure 7. Comparison Ratio of anchor break-out factors in clay

3.3 Effect of overburden pressure

Effect of overburden pressure $N_{c\gamma}$ in clay on anchor pullout capacity is shown in Fig. 8. The Effect of overburden pressure $N_{c\gamma}$ increase with a peak at at H/D ≈ 7. The $N_{c\gamma}$ is accounted for 15.7 for circular anchor, 21.8 for star A anchor, and 17.2 for star B anchor. This finding show differences with Merifield et. al (2003) in which the $N_{c\gamma}$ has a maximum at H/D ≈ 7, and it si approximately 13.9 for circular anchor. Meyerhof et. al (1968) suggested the effect of overburden pressure $N_{c\gamma}$ increase linearly.

Experimental laboratory tests by Djamaluddin et al. (2013) suggested that the effect of overburden pressure $N_{c\gamma}$ increases until a maximum value at H/D ≈ 7, and its value is about 15.4 for circular anchor, 21.8 for star A anchor, and 16.8 for star B anchor.

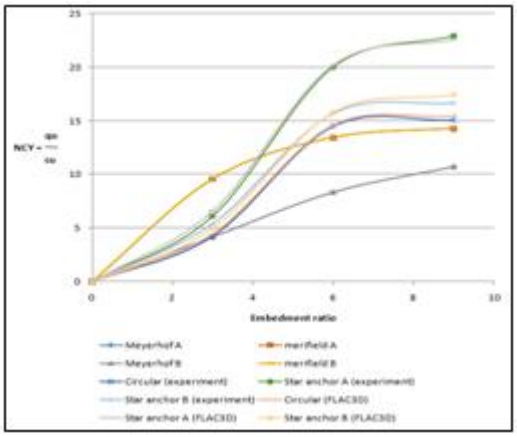

Figure 8. Comparison Effect of overburden pressure anchors in clay

IV. CONCLUSIONS

1. As it is expected, the break-out factor for Star A and star B anchors in weightless soil are always greater than those obtained for circular anchors at corresponding embedment ratios.
2. A comparison of numerical geomechanics analysis in finite difference approach with those published from small scale laboratory tests show well agreement.
3. The ultimate capacity for all anchors was found to increase linearly with overburden pressure up to a limiting value. This confirms that the principle of superposition is valid for shallow circular, Star A, and star B anchors. The limiting value reflect the transition from shallow to deep anchors behavior where the mode of failure becomes localized around the anchor. At a given embedment depth an anchor may behave as shallow or deep, depending on the dimensionless overburden ratio $\gamma H/c_u$.
4. The ultimate capacity of circular, Star A, and star B anchors is not likely to be affected noticeably by anchor roughness. The computed reduction in the ultimate capacity between rough and smooth anchors was typically less than 2%.

REFERENCES

[1] Djamaluddin, A.R., Arsyad, A., Maricar, I., Samang, L., Oemar, I., Burhan, I. 2013. Experimental Study of Pullout Capacity of Star Plate Anchor . Proceeding of 7th International Conference on Asia and Pacific Coasts (APAC 2013) Bali, Indonesia.

[2] Itasca. 2005. Theory and Background of FLAC3D.
[3] Merifield, R. S., Lyamin, A. V., Sloan, S. W. & Yu, H. S. 2003. Three-Dimensional Lower Bound Solutions for Stability of Plate Anchors in Clay. Journal of Geotechnical and Geo environmental Engineering, ASCE, 129(3), pp: 243-253.
[4] Merifield, R. S., Lyamin, A. V. and Sloan, S. W. 2005. The Stability of Inclined Plate Anchors in Purely Cohesive Soil. Journal of Geotechnical and Geo environmental Engineering, ASCE, 131(6), pp: 792-799.
[5] Meyerhof, G. G. and Adams, J. I. 1968. The Ultimate Uplift Capacity of Foundations. Canadian Geotechnical Journal, 24(4), pp: 589-592.
[6] Rowe, R. K. and Davis, E. H. 1982. The Behavior of Anchor Plates in Clay. Geotechnique, 32(1), pp: 9-23.